Coupled-Wave Small-Signal Transient Analysis of GaAs Distributed Amplifier

KELI HAN, STUDENT MEMBER, IEEE, AND THOMAS T. Y. WONG, MEMBER, IEEE

Abstract—**A coupled-wave small-signal transient analysis for the GaAs distributed amplifier is presented. The analysis takes into consideration the effect of c_{dg} in the active device, leading to a coupled-mode formulation. Dispersions within the transmission lines and the presence of two normal modes make it impractical to obtain broad-band matching. Numerical results for specific terminations and various degrees of passive and active coupling clearly indicate the influence of c_{dg} and the necessity for coupled-mode analysis. The presented numerical scheme based on Bromwich integration can be incorporated into CAD routines for time-domain response optimization.**

I. Introduction

THE POTENTIAL of the distributed amplifier in waveform amplification has long been visualized. Indeed, the search for a high-performance pulse amplifier for radar systems was one of the motivations that led to the development of the first distributed amplifier [1], [2]. Since then, considerable effort has been devoted to the frequency-domain analysis and measurement of the distributed amplifier [3]–[14]. An early time-domain investigation carried out from the network viewpoint [15], as well as more recent experimental studies [6], [8], have provided much insight into the time-domain aspect of distributed amplification. An accurate analysis of the distributed amplifier in the time domain is a formidable task, since it is necessary to take into account such factors as the nonlinearity of the device, the presence of coupled waves, and reflections arising from load mismatch.

In this paper, we address the time-domain wave propagation aspect of the distributed amplifier by means of a small-signal coupled-mode analysis. A transient analysis of passive coupled-mode systems in general has been given by Barnes [16]. The distributed amplifier, however, has both passive and active coupling. Furthermore, the active coupling is nonreciprocal. Nevertheless, one can represent the amplifier using the general coupled-wave system shown in Fig. 1. The two transmission lines, representing the gate line and the drain line in the context of the GaAs distributed amplifier, are uniformly coupled to each other by a distributed active two-port network. Such a representation is a good approximation to the actual amplifier when the phase shift between adjacent stages is small. In the present analysis, it is more convenient to use y parameters of the distributed two-port which represents the active device. As the lengths of the transmission lines are not the same in most cases, two linear coordinates z and z' have to be introduced. Because of the nature of the loading effect by the active device, it is not possible to obtain a broad-band match for the two lines. On the other hand, the amplifier is terminated at both the drain and gate lines in order to function and interface with external circuits. The effects of the termination mismatch as well as that of the coupling circuit are considered in subsequent discussions. The small-signal nature of the analysis permits the use of transform techniques, so that the transient response can be derived from the frequency-domain analysis by the inverse Laplace transform.

Manuscript received January 30, 1989; revised July 26, 1989.

The authors are with the Department of Electrical and Computer Engineering, Illinois Institute of Technology, Chicago, IL 60616.

IEEE Log Number 8931558.

II. Theory

The usual transmission line analysis in the frequency domain applied to the system shown in Fig. 1 yields the following equations:

$$\frac{dV_1}{dz} = -Z_1 I_1$$

$$\frac{dI_1}{dz} = -(Y_1 + Y_{11})V_1 - Y_{12}V_2 \tag{1}$$

and

$$\frac{dV_2}{dz'} = -Z_2 I_2$$

$$\frac{dI_2}{dz'} = -Y_{21}V_1 - (Y_2 + Y_{22})V_2 \tag{2a}$$

where Z_1, Z_2 and Y_1, Y_2 are the impedances and admittances per unit length of lines 1 and 2, respectively. Y_{11}, Y_{12}, Y_{21}, and Y_{22} are the per-unit-length y parameters of the distributed two-port network.

It is convenient to rescale the coordinate for line 2 so that equations (2a) read

$$\frac{dV_2}{dz} = -\left(\frac{d_2}{d_1}\right) Z_2 I_2$$

$$\frac{dI_2}{dz} = -\left(\frac{d_2}{d_1}\right) Y_{21}V_1 - \left(\frac{d_2}{d_1}\right)(Y_2 + Y_{22})V_2. \tag{2b}$$

0018-9480/90/0100-0023$01.00

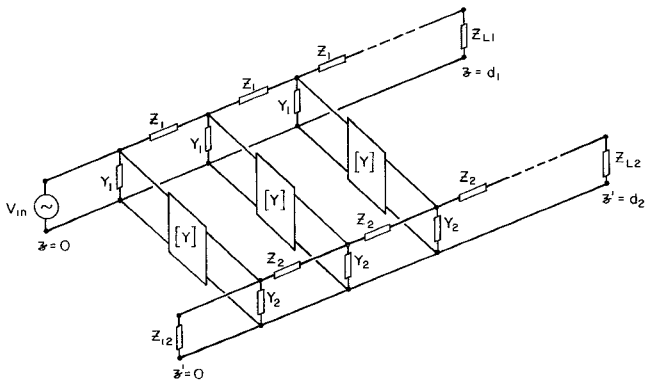

Fig. 1. A general coupled-wave system represented as two transmission lines coupled by a distributed two-port network.

After some mathematical manipulation, the following coupled-wave equations are obtained:

$$\frac{d^2V_1}{dz^2} = \gamma_{11}^2 V_1 + \gamma_{12}^2 V_2$$

$$\frac{d^2V_2}{dz^2} = \gamma_{21}^2 V_1 + \gamma_{22}^2 V_2 \tag{3}$$

where

$$\gamma_{11}^2 = Z_1(Y_1 + Y_{11})$$

$$\gamma_{12}^2 = Z_1 Y_{12}$$

$$\gamma_{21}^2 = \left(\frac{d_2}{d_1}\right)^2 Z_2 Y_{21}$$

$$\gamma_{22}^2 = \left(\frac{d_2}{d_1}\right)^2 Z_2(Y_2 + Y_{22}). \tag{4}$$

By eliminating either V_1 or V_2 in (3) and solving the resulting fourth-order linear differential equations, we finally obtain the voltage expressions in both transmission lines as follows:

$$V_1 = A_1 e^{-\gamma_1 z} + B_1 e^{\gamma_1 z} + C_1 e^{-\gamma_2 z} + D_1 e^{\gamma_2 z}$$

$$V_2 = A_2 e^{-\gamma_1 z} + B_2 e^{\gamma_1 z} + C_2 e^{-\gamma_2 z} + D_2 e^{\gamma_2 z} \tag{5}$$

where

$$\gamma_{1,2} = \left\{ \frac{1}{2}\left[(\gamma_{11}^2 + \gamma_{22}^2) \pm \left[(\gamma_{11}^2 + \gamma_{22}^2) - 4(\gamma_{11}^2\gamma_{22}^2 - \gamma_{12}^2\gamma_{21}^2) \right]^{1/2} \right] \right\}^{1/2} \tag{6}$$

and when $c_{dg} = 0$, $\gamma_1 = \gamma_{11}$, $\gamma_2 = \gamma_{22}$, and $\gamma_{12} = \gamma_{21} = 0$.

From (5) it is seen that in general there exist two types of waves with different propagation constants in both lines. The coefficients A_i, B_i, C_i, and D_i satisfy the following four relations, which can be obtained from (3):

$$A_2 = \left(\frac{\gamma_1^2 - \gamma_{11}^2}{\gamma_{12}^2}\right) A_1 = \left(\frac{\gamma_{21}^2}{\gamma_1^2 - \gamma_{22}^2}\right) A_1$$

$$B_2 = \left(\frac{\gamma_1^2 - \gamma_{11}^2}{\gamma_{12}^2}\right) B_1 = \left(\frac{\gamma_{21}^2}{\gamma_1^2 - \gamma_{22}^2}\right) B_1$$

$$C_2 = \left(\frac{\gamma_2^2 - \gamma_{11}^2}{\gamma_{12}^2}\right) C_1 = \left(\frac{\gamma_{21}^2}{\gamma_2^2 - \gamma_{22}^2}\right) C_1$$

$$D_2 = \left(\frac{\gamma_2^2 - \gamma_{11}^2}{\gamma_{12}^2}\right) D_1 = \left(\frac{\gamma_{21}^2}{\gamma_2^2 - \gamma_{22}^2}\right) D_1. \tag{7}$$

For the model shown in Fig. 1, the boundary conditions are taken to be as follows:

$$V_1(0, s) = V_{in} \qquad V_1(d_1, s) = Z_{l1} I_1(d_1, s)$$
$$V_2(0, s) = -Z_{i2} I_2(0, s) \qquad V_2(d_1, s) = Z_{l2} I_2(d_1, s). \tag{8}$$

Using the relations in (7) and the boundary conditions in (8), we have the following matrix equation for coefficients A_1, B_1, C_1, and D_1:

$$\begin{bmatrix} G_{11} & G_{12} & G_{13} & G_{14} \\ G_{21} & G_{22} & G_{23} & G_{24} \\ G_{31} & G_{32} & G_{33} & G_{34} \\ G_{41} & G_{42} & G_{43} & G_{44} \end{bmatrix} \begin{bmatrix} A_1 \\ B_1 \\ C_1 \\ D_1 \end{bmatrix} = \begin{bmatrix} V_{in} \\ 0 \\ 0 \\ 0 \end{bmatrix} \tag{9}$$

where

$$G_{11} = G_{12} = G_{13} = G_{14} = 1$$

$$G_{21} = \left(1 - \frac{Z_{l1}}{Z_1}\gamma_1\right) e^{-\gamma_1 d_1} \qquad G_{22} = \left(1 + \frac{Z_{l1}}{Z_1}\gamma_1\right) e^{\gamma_1 d_1}$$

$$G_{23} = \left(1 - \frac{Z_{l1}}{Z_1}\gamma_2\right) e^{-\gamma_2 d_1} \qquad G_{24} = \left(1 + \frac{Z_{l1}}{Z_1}\gamma_2\right) e^{\gamma_2 d_1}$$

$$G_{31} = \left(\frac{\gamma_1^2 - \gamma_{11}^2}{\gamma_{12}^2}\right)\left(1 + \frac{Z_{i2}}{Z_b}\gamma_1\right)$$

$$G_{32} = \left(\frac{\gamma_1^2 - \gamma_{11}^2}{\gamma_{12}^2}\right)\left(1 - \frac{Z_{i2}}{Z_b}\gamma_1\right)$$

$$G_{33} = \left(\frac{\gamma_2^2 - \gamma_{11}^2}{\gamma_{12}^2}\right)\left(1 + \frac{Z_{i2}}{Z_b}\gamma_2\right)$$

$$G_{34} = \left(\frac{\gamma_2^2 - \gamma_{11}^2}{\gamma_{12}^2}\right)\left(1 - \frac{Z_{i2}}{Z_b}\gamma_2\right)$$

$$G_{41} = \left(\frac{\gamma_1^2 - \gamma_{11}^2}{\gamma_{12}^2}\right)\left(1 - \frac{Z_{l2}}{Z_b}\gamma_1\right) e^{-\gamma_1 d_1}$$

$$G_{42} = \left(\frac{\gamma_1^2 - \gamma_{11}^2}{\gamma_{12}^2}\right)\left(1 + \frac{Z_{l2}}{Z_b}\gamma_1\right) e^{\gamma_1 d_1}$$

$$G_{43} = \left(\frac{\gamma_2^2 - \gamma_{11}^2}{\gamma_{12}^2}\right)\left(1 - \frac{Z_{l2}}{Z_b}\gamma_2\right) e^{-\gamma_2 d_1}$$

$$G_{44} = \left(\frac{\gamma_2^2 - \gamma_{11}^2}{\gamma_{12}^2}\right)\left(1 + \frac{Z_{l2}}{Z_b}\gamma_2\right) e^{\gamma_2 d_1} \tag{10}$$

and

$$Z_b = \frac{d_2}{d_1} Z_2.$$

With $[G]$ being nonsingular, A_1, B_1, C_1, and D_1 can be obtained by solving (9), which gives A_2, B_2, C_2, and D_2 from (7). The output voltage $V_o(s)$ is then given by

$$V_o(s) = A_2 e^{-\gamma_1 d_1} + B_2 e^{\gamma_1 d_1} + C_2 e^{-\gamma_2 d_1} + D_2 e^{\gamma_2 d_1}. \quad (11)$$

The time-domain response of the output voltage is thus obtained from the inverse Laplace transform of $V_o(s)$. The inverse Laplace transform can be obtained by evaluating the Bromwich integral numerically [17]:

$$V_o(t) = \frac{1}{2\pi j} \int_{B_r} V_o(s) e^{st}\, ds$$

$$\approx \frac{1}{2\pi} \sum_{n=-M}^{M} V_o(\sigma + jn\Delta\omega) e^{(\sigma + jn\Delta\omega)t} \Delta\omega \quad (12)$$

for suitably chosen σ and $\Delta\omega$ and a sufficiently large M.

III. Numerical Results

The derivation of voltage waves in the coupled transmission line pair is readily applicable to the distributed amplifier when the properly normalized two-port equivalent circuit of a GaAs FET as shown in Fig. 2 is substituted for the coupling network in Fig. 1. Only the most essential elements reflecting the intrinsic properties of a typical MESFET are included in the equivalent circuit. Other contributions arising from device periphery which are more specific to a particular circuit pattern are not taken into consideration. Nevertheless, the y-parameter representation can easily be made to accommodate additional circuit components when their values are available from a given design. The elements which provide coupling between the two lines are c_{dg} and g_m. However, their effects are quite different since c_{dg} is passive and reciprocal, while g_m is active and nonreciprocal. Assuming typical MESFET parameters and interstage spacing for the gate line and the drain line, one arrives at the following y parameters:

$$Y_{11} = \frac{1}{l_g}\left(\frac{j\omega c_{gs}}{1 + j\omega c_{gs} r_g} + j\omega c_{dg}\right)$$

$$Y_{12} = \frac{1}{l_g}(-j\omega c_{dg})$$

$$Y_{21} = \frac{1}{l_d}\left(\frac{g_m}{1 + j\omega c_{gs} r_g} - j\omega c_{dg}\right)$$

$$Y_{22} = \frac{1}{l_d}\left[\frac{1}{r_d} + j\omega(c_{dg} + c_{ds})\right] \quad (13)$$

where the numerical values of $r_g = 1.3\ \Omega$, $c_{gs} = 1.24$ pF, $g_m = 53$ mmho, $r_d = 800\ \Omega$, $c_{ds} = 0.24$ pF, $c_{dg} = 0.028$ pF, $l_g = 0.7$ mm, and $l_d = 1.21$ mm are used for the calculations presented in subsequent diagrams. The two transmission lines are both with 100 Ω characteristic impedances when the coupling network is absent.

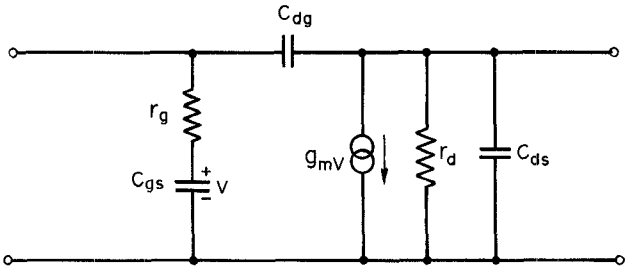

Fig. 2. Small-signal equivalent circuit for a GaAs MESFET.

Although the theme of this investigation is the small-signal transient response of the amplifier, it is of interest to consider the frequency-domain characteristics in order to gain some insight into the interpretation of time-domain results. When c_{dg} is absent, there exist only the so-called cold modes in each line and only one wave in the gate line. When c_{dg} is present, two waves will exist in both lines so that two characteristic impedances can be defined for each line, i.e.,

$$Z_{011} = \frac{Z_1}{\gamma_1} \qquad Z_{012} = \frac{Z_1}{\gamma_2}$$

$$Z_{021} = \frac{Z_2}{\gamma_1} \quad \text{and} \quad Z_{022} = \frac{Z_2}{\gamma_2}. \quad (14)$$

These impedances correspond to the "fast and slow" wave characteristic impedances as defined in [5]. We define Z_{011} and Z_{022} as characteristic impedances of dominant modes in gate line and drain line, respectively, since the two impedances tend to the intrinsic impedance of each line when c_{dg} approaches zero. These characteristic impedances are not equal and have different frequency dependence. In view of the fact that it is not possible to provide a broad-band matched load to both modes in the lines, a more realistic arrangement would be to terminate each line with the real part of the characteristic impedance of the dominant mode at midband frequency. The effects of c_{dg} on the characteristic impedances of the two waves are shown in Fig. 3. Owing to the loading effect of the FET, considerable dispersion is observed in the imaginary part of these impedances even when c_{dg} is absent. The presence of c_{dg} together with g_m further intensifies the variation of characteristic impedances with respect to frequency. On the other hand, considerable dispersion is observed only in the real part of the propagation constant, which is considerably smaller in magnitude than the imaginary part, as shown in Fig. 4. Of particular interest is the observation of α_1 becoming negative when the coupling between the two lines is significant. This is observed only when coupled mode analysis is considered. A negative α signifies the intrinsic growth in the amplitude of the wave along the direction of propagation. However, this is not a necessary condition for amplification, as power gain can be achieved through the action of the transconductance g_m. This can readily be verified by considering the case when c_{dg} is zero so that α is positive for both modes; voltage and current gain (from generator to load) of con-

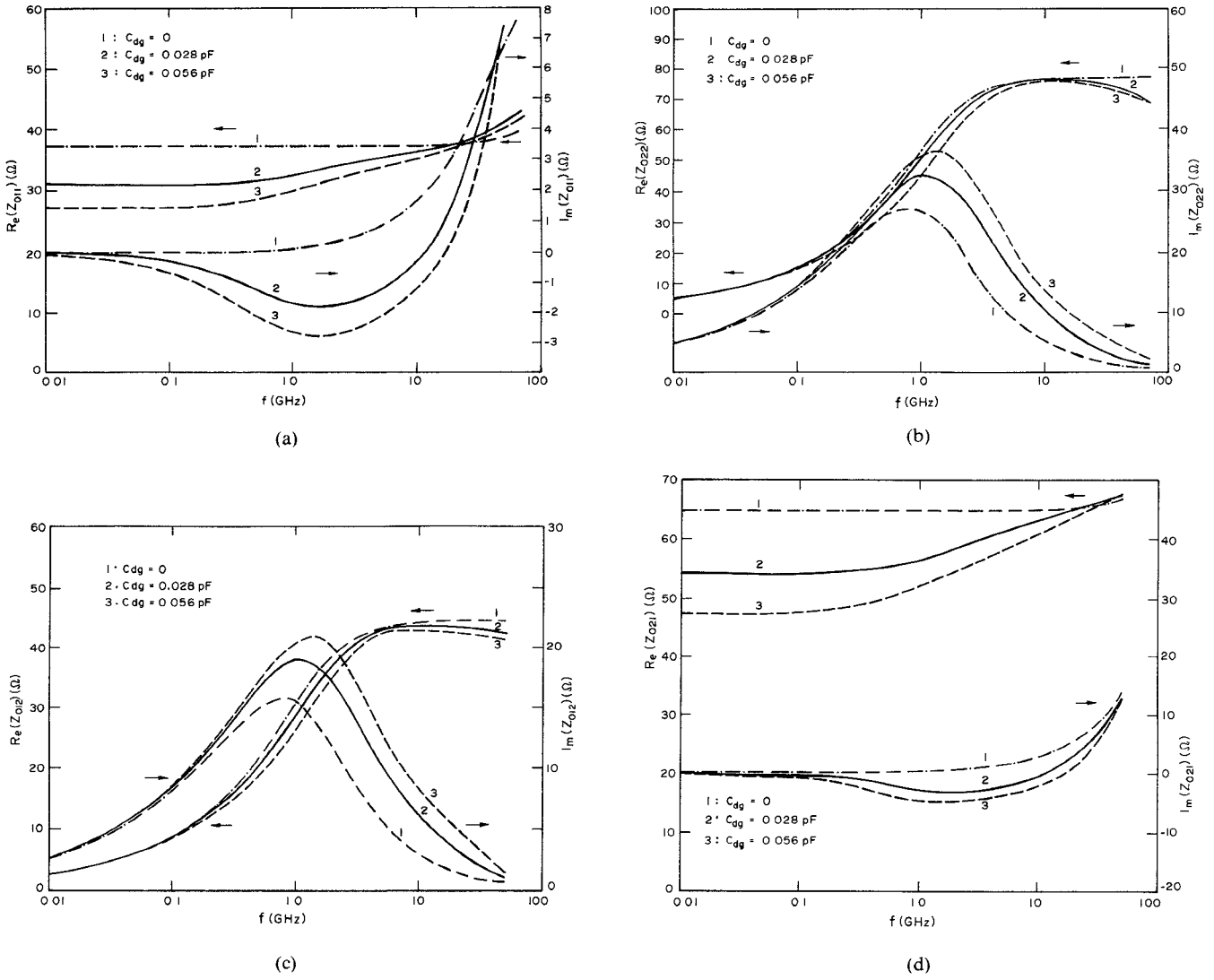

Fig. 3. Frequency dependence of the characteristic impedances of the different waves: (a) Z_{011}, (b) Z_{022}, (c) Z_{012}, (d) Z_{021}.

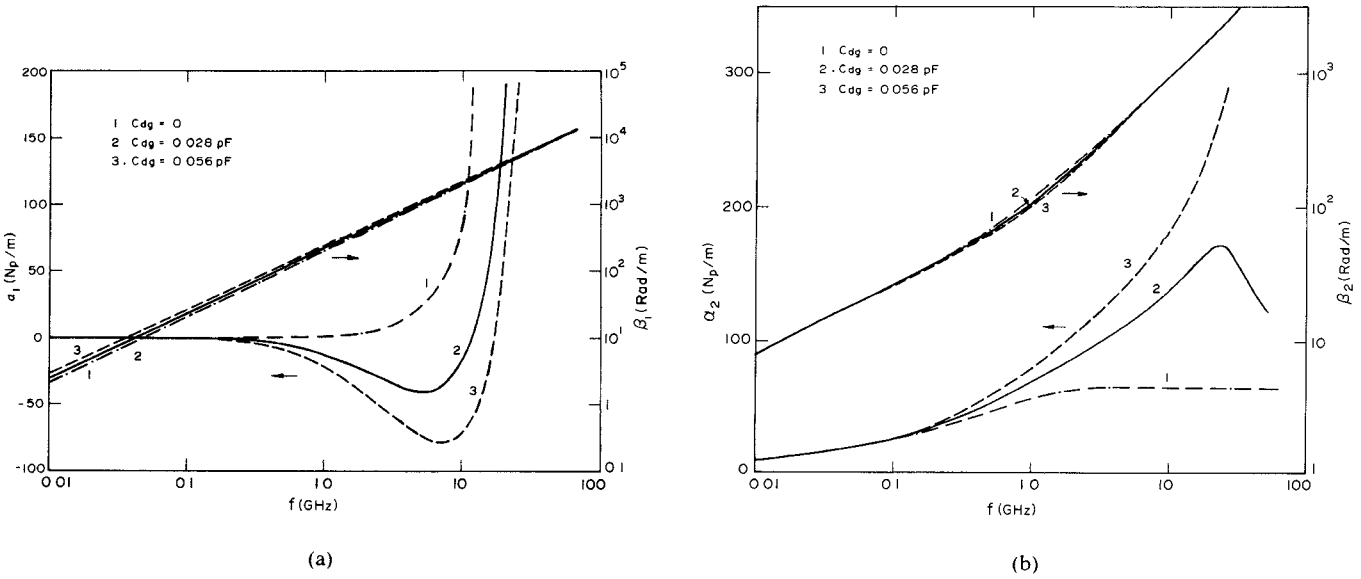

Fig. 4. Propagation constants γ_1 and γ_2 versus frequency for different c_{dg} and g_m (*continued on next page*).

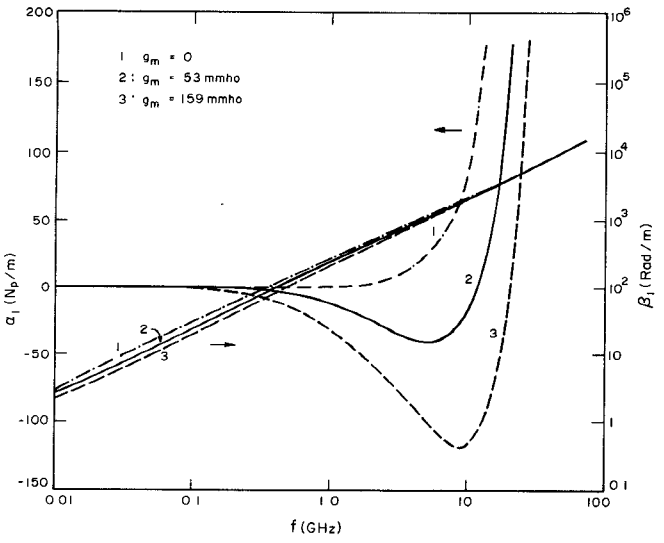

(c)

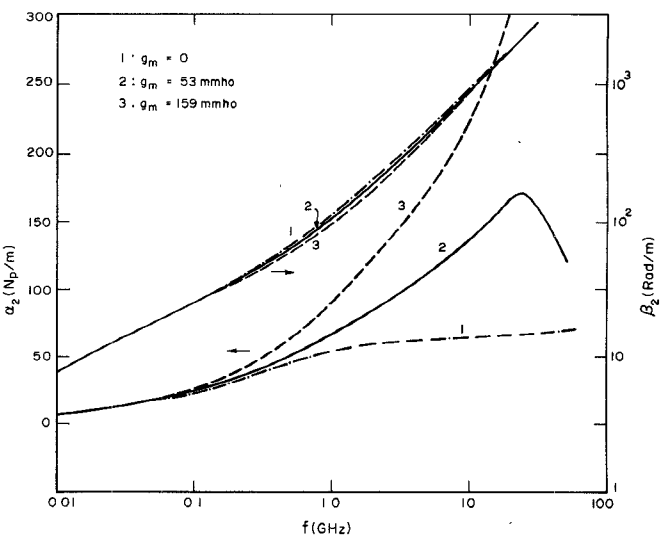

(d)

Fig. 4. (*Continued*).

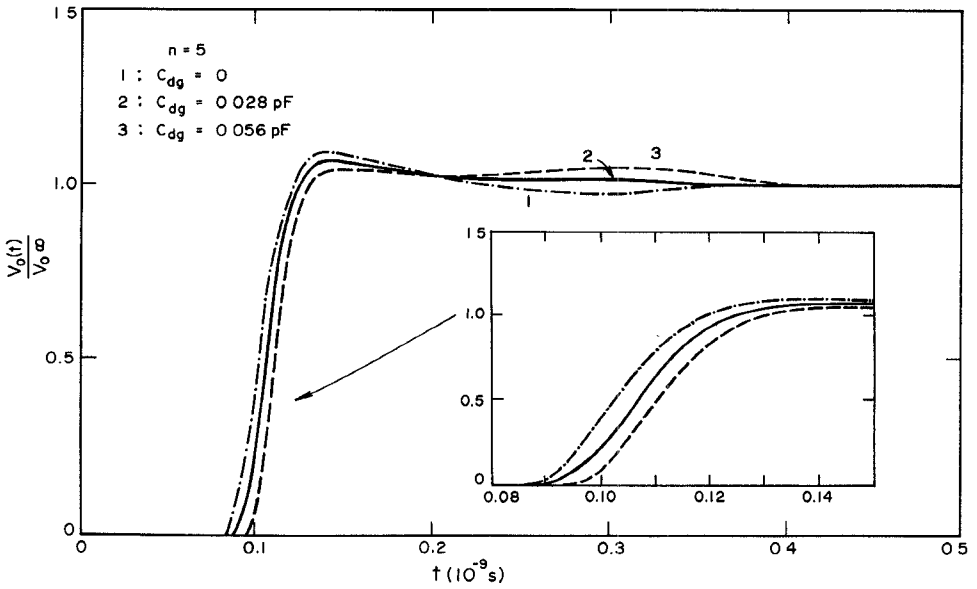

Fig. 5. Transient response of a five-stage MESFET distributed amplifier with different c_{dg}.

siderable magnitude can still be obtained. With both modes present, the voltage and current waves in each line comprise four linearly independent waves, two in each direction of propagation.

To obtain the small-signal transient response, we assume that the input end of the gate line is excited by a unit-step voltage. For calculations carried out in this investigation, the termination for the gate line was taken to be 35 Ω and that for the drain line was taken to be 75 Ω, which correspond to the characteristic impedances of $35.18 - j1.34$ Ω and $74.71 + j17.76$ Ω of the dominant mode in each line at 5 GHz, representing approximately half of the 3 dB bandwidth. Using the method described in Section II, the normalized transient output voltage was calculated for different coupling elements c_{dg} and g_m, as shown in Fig. 5 and Fig. 6. It can be observed that both c_{dg} and g_m have influence on the overall transient response of the amplifier. The amount of overshoot observed in this calculation, however, is not severe, since the overall lengths of the two transmission lines are not large enough to permit the manifestation of multiple reflection. For a response curve with little overshoot and ringing, it is meaningful to define the rise time as the duration for the system output to go from 10 to 90 percent of the steady-state value. The rise times for amplifiers with different numbers of stages are shown in Fig. 7, which clearly indicates the effect of coupled waves induced by c_{dg} on the time-domain response of the distributed amplifier.

The numerical Bromwich integration employed in this investigation can serve as a basis for time-domain response optimization in CAD routines. All the calculations presented in this section were carried out using the model given in Fig. 1. However, for certain more complicated coupling networks, the use of a high-frequency asymptotic

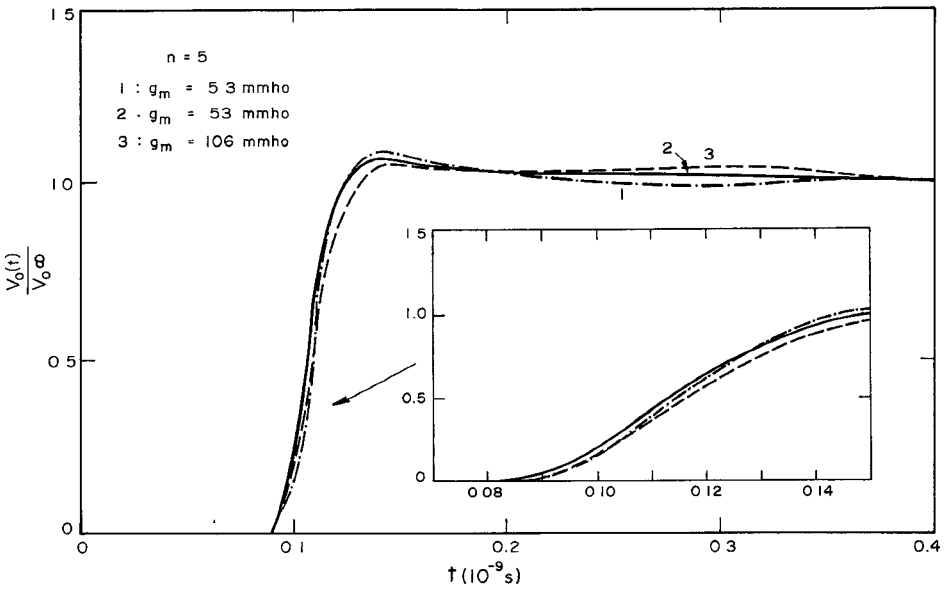

Fig. 6. Transient response of a five-stage MESFET distributed amplifier with different g_m.

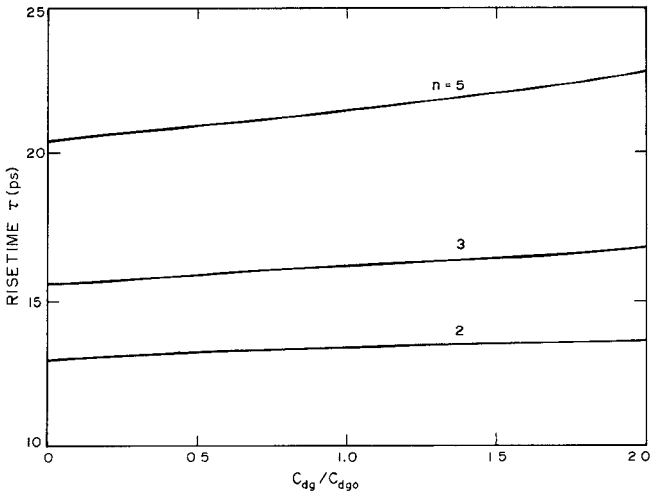

(a)

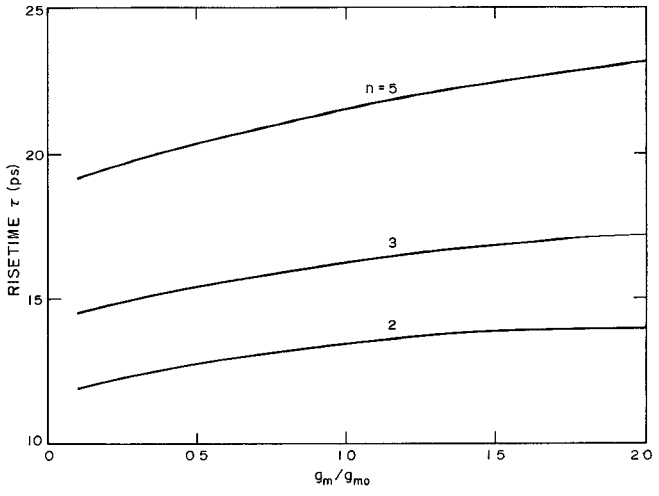

(b)

Fig. 7. (a) Dependence of rise time on c_{dg} for different distributed amplifiers ($c_{dg0} = 0.028$ pF). (b) Dependence of rise time on g_m for different distributed amplifiers ($g_{m0} = 53$ mmho).

model in the large-$|s|$ portion of the contour can speed up the computation process considerably.

IV. Conclusion

A small-signal transient analysis of the GaAs distributed amplifier has been carried out with the objective of assessing the influence of coupled waves on the time-domain performance. With the aid of a model system represented by a pair of transmission lines coupled uniformly to each other by a distributed two-port network characterized by y parameters, the transient response was obtained by numerical evaluation of the Bromwich integral for the inverse Laplace transform. The presence of two propagation modes in each line along with the frequency dependence of the corresponding characteristic impedances makes it impractical to provide broad-band matched terminations. As a compromise, one may choose to terminate the lines with a load corresponding to the resistive part of the characteristic impedance of the dominant wave at midband frequency. Numerical results clearly reveal the effect of coupled waves on the time-domain response, thus indicating the necessity of including c_{dg} in the analysis. The formulation presented can also be applied to the transient analysis of distributed systems and devices with coupled wave interactions.

References

[1] W. S. Percival, "Thermionic valve circuits," U.K. Patent 460562, Jan. 1937.

[2] E. L. Ginzton, W. R. Hewlett, J. H. Jasberg and J. D. Noe, "distributed amplification," *Proc. IRE*, vol. 36, pp. 956–969, Aug. 1948.

[3] G. W. McIver, "A traveling-wave transistor," *Proc. IEEE*, vol. 53, pp. 1747–1748, Nov. 1965.

[4] E. H. Kopp, "A coupled mode analysis of the traveling wave transistor," *Proc. IEEE*, vol. 54, pp. 1571–1572, Nov 1966.

[5] W. Jutzi, "Uniform distributed amplifier analysis with fast and slow waves," *Proc. IEEE*, vol. 56, pp. 66–67, Jan. 1968.

[6] F. Meyer, "Wide-band pulse amplifier," *IEEE J. Solid-State Circuits*, vol. SC-13, pp. 409–411, June 1978.
[7] Y. Ayasli, R. L. Mozzi, J. L. Vorhaus, L. D. Reynolds, and R. A. Pucel, "A monolithic GaAs 1–13 GHz traveling wave amplifier," *IEEE Trans. Microwave Theory Tech.*, vol. MTT-30, pp. 976–981, July 1982.
[8] E. W. Strid and K. R. Gleason, "A dc–12 GHz monolithic GaAs FET distributed amplifier," *IEEE Trans. Microwave Theory Tech.*, vol. MTT-30, pp. 969–975, July 1982.
[9] K. B. Niclas, W. T. Wilser, T. R. Kritzer, and R. R. Pereira, "On theory and performance of solid-state microwave distributed amplifier," *IEEE Trans. Microwave Theory Tech.*, vol. MTT-31, pp. 447–456, June 1983.
[10] J. B. Beyer, S. N. Prasad, R. C. Becker, J. E. Nordman, and G. K. Hohenwarter, "MESFET distributed amplifier design guidelines," *IEEE Trans. Microwave Theory Tech.*, vol. MTT-32, pp. 268–275, Mar. 1984.
[11] A. J. Holden, D. R. Daniel, I. Davies, C. H. Oxley, and H. D. Rees, "Gallium arsenide traveling wave field effect transistors," *IEEE Trans. Electron Devices*, vol. ED-32, pp. 61–66, Jan. 1985.
[12] R. A. Larue, S. G. Bandy, and G. A. Zdasiuk, "A 12-dB high gain monolithic distributed amplifier," *IEEE Trans. Electron Devices*, vol. ED-33, pp. 2073–2078, Dec. 1986.
[13] T. McKay, J. Eisenberg, and R. E. Williams, "A high performance 2–18.5 GHz distributed amplifier—Theory and experiment," *IEEE Trans. Electron Devices*, vol. ED-33, pp. 2090–2099, Dec. 1986.
[14] W. Heinrich, "Distributed equivalent-circuit model for traveling wave FET design," *IEEE Trans. Microwave Theory Tech.*, vol. MTT-35, pp. 487–491, May 1987.
[15] W. K. Chen, "Distributed amplification: A new approach," *IEEE Trans. Electron Devices*, vol. ED-14, pp. 215–221, Apr. 1967.
[16] C. W. Barnes, "On the impulse response of a coupled-mode system," *IEEE Trans. Microwave Theory Tech.*, vol. MTT-13, pp. 432–435, July 1965.
[17] T. Wong, "Gate-width dependence of GaAs FET transient response," *IEEE Electron Device Lett.*, vol. EDL-6, pp. 146–148, Mar. 1985.

✠

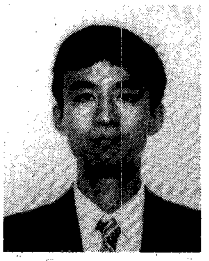

Keli Han (S'89) was born in Changsha, China, on November 9, 1959. He received the B.S. and M.S. degrees from the Chengdu Institute of Radio Engineering, Chengdu, China, in 1981 and 1984, respectively. He is currently working toward the Ph.D. degree in electrical engineering at the Illinois Institute of Technology, Chicago, IL, where he is a teaching assistant. His research interests include electromagnetic wave propagation, semiconductor device theory, and computation methods.

✠

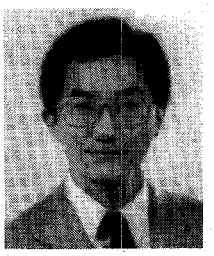

Thomas T. Y. Wong (S'74–M'80) was born in 1952. He received the B.Sc. (Eng.) degree from the University of Hong Kong in 1975 and the M.S. and Ph.D. degrees from Northwestern University in 1978 and 1980, respectively.

From 1975 to 1976 he was a Product Engineer at Motorola Semiconductor, Inc., responsible for small-signal semiconductor devices in the Asia–Pacific region. He was a Teaching Assistant from 1976 to 1978, and a Research Assistant from 1978 to 1980, in the Department of Electrical Engineering and Computer Science at Northwestern University, Evanston, IL, where he was the major participant in establishing the Microwave Characterization Laboratory. He carried out transport and dielectric studies on ionic conductors, polymers, and ceramics and was a Research Fellow at the Materials Research Center until September 1981, when he joined the Illinois Institute of Technology, Chicago, IL, where he is now Associate Professor and Director of the Graduate Program in Electrical and Computer Engineering. His research activities have focused on transient phenomena and high-speed devices.

Dr. Wong has served as Chairman (1987–1988) of the Chicago Joint Chapter of Antennas and Propagation and Microwave Theory and Techniques Societies. He is also a member of the American Physical Society,